

Stress-Strain Response and Dilatancy of Sandy Gravel in Triaxial Compression and Plane Strain

Andrew Strahler, S.M.ASCE¹; Armin W. Stuedlein, Ph.D., P.E., M.ASCE²;
and Pedro W. Arduino, Ph.D., P.E., M.ASCE³

Abstract: The strength and stress-dilatancy of uniform sands has been studied extensively in geotechnical investigations, and practitioners can draw on a wealth of previously reported data for the estimation of their volumetric response. However, the suitability of accepted stress-dilatancy theory and empiricism has not been evaluated for well-graded gravelly soils. Axisymmetric, isotropically consolidated drained compression, and pure shear, plane strain quasi- K_0 consolidated drained tests were performed on well-graded Kanaskat gravel using confining pressures ranging over three orders of magnitude to determine its stiffness, strength, and stress-dilatancy response. The plane strain stiffness, strength, and stress-dilatancy of Kanaskat gravel is observed from tests performed using a large cubical true-triaxial device with flexible bladders. The observed response is interpreted with a view of experimental boundary conditions and their impact on the volumetric response. The observed plane strain shear modulus and friction, and dilation angles of well-graded sandy gravel soils commonly used in practice are significantly higher than those measured in the triaxial compression stress path. Existing empirical and modified stress-dilatancy expressions proposed for low confining pressures underestimate the observed dilation response; however, another common empirical approach appears to adequately capture the dilatancy. The data reported herein should help practitioners estimate plane strain behavior of sandy gravel mixtures. DOI: 10.1061/(ASCE)GT.1943-5606.0001435. © 2015 American Society of Civil Engineers.

Introduction

Soil dilatancy was initially investigated by Reynolds (1885) and has since been recognized to control critical aspects of soil behavior at working stresses. Although the stability of slopes or shallow foundations, geotechnical structures that lie in proximity to free surfaces, are less affected by soil dilation (Zienciewicz et al. 1975), the serviceability of highly confined geotechnical elements such as tunnels and deep foundations is greatly impacted by soil dilatancy (Houlsby 1991). Rowe (1962) and Poorooshasb and Roscoe (1961) presented two stress-dilatancy relationships for granular soils based on laboratory investigations on Fort Peck sand by Taylor (1948) using assumed uniform particle sizes and packing. Building on Rowe's work, a significant body of literature has been developed on the stress-dilatancy behavior of uniform sands (Cornforth 1964; Lee and Seed 1967; Rowe 1969; Tatsuoka 1976; Bolton 1986; Chu 1994; Schanz and Vermeer 1996; Panda and Ghosh 2000; Hanna 2001; Wan and Guo 2004; Chakraborty and Salgado 2010). A widely used empirical stress-dilatancy relationship developed by Bolton (1986) and focused on the strength parameters of uniform sands yielded

$$\phi'_f = \phi'_{cv} + a\psi_f \quad (1)$$

¹Graduate Research Assistant, School of Civil and Construction Engineering, Oregon State Univ., 101 Kearney Hall, Corvallis, OR 97331.

²Associate Professor, School of Civil and Construction Engineering, Oregon State Univ., 101 Kearney Hall, Corvallis, OR 97331 (corresponding author). E-mail: Armin.Stuedlein@oregonstate.edu

³Professor, Dept. of Civil and Environmental Engineering, Univ. of Washington, 201 More Hall, P.O. Box 352700, Seattle, WA 98195-2700.

Note. This manuscript was submitted on November 18, 2014; approved on September 17, 2015; published online on December 22, 2015. Discussion period open until May 22, 2016; separate discussions must be submitted for individual papers. This paper is part of the *Journal of Geotechnical and Geoenvironmental Engineering*, © ASCE, ISSN 1090-0241.

where ϕ'_f = friction angle at failure; ϕ'_{cv} = friction angle at a constant volume condition; and coefficient a varies based on soil type and stress path. The dilation angle at failure, ψ_f , in Eq. (1) is defined by

$$\sin \psi_f = \frac{-(d\varepsilon_v/d\varepsilon_1)_f}{2 - (d\varepsilon_v/d\varepsilon_1)_f} \quad (2)$$

where $d\varepsilon_v$ and $d\varepsilon_1$ = changes in the volumetric and axial strains during shearing; and subscript f = failure. Although the various theories and empirical relationships work well in many cases, they are based on stress-dilatancy relations developed assuming uniform particle packing and have not been validated against the response of well-graded granular soils. The study of the stress-strain response of well-graded gravelly soils to date consists of in situ direct shear tests, limited ranges in confining pressure, or large, angular, and weak rock fill that exhibit extensive particle breakage (Holtz and Gibbs 1956; Marsal 1967; Skermer and Hillis 1970; Marachi et al. 1972; Charles and Watts 1980; Matsuoka and Liu 1998; Matsuoka et al. 2001; Zhao et al. 2013; Xiao et al. 2014). The aim of this study is to characterize the uniaxial and plane strain behavior of Kanaskat gravel, a rounded to subrounded well-graded sandy gravel used to construct several tall mechanically stabilized earth (MSE) walls in SeaTac, WA, described by Stuedlein et al. (2007, 2010, 2012). A series of large, axisymmetric, isotropically-consolidated drained triaxial compression (AICD) and cubical, pure shear, quasi- K_0 consolidated drained plane strain (PSK₀CD) tests were conducted on Kanaskat gravel to study the influence of stress path on its stiffness, strength, and stress-dilatancy response. This paper first details the comprehensive laboratory testing program that was used to investigate the stress-strain response of Kanaskat gravel. The stress-strain-strength and volume change behavior observed in large axisymmetric triaxial tests over a wide range of confining stresses is provided as a baseline response. Then, the highly frictional stress-strain-strength and volume change response of quasi- K_0 consolidated plain strain pure shear tests are described,

in consideration of complex boundary conditions and shear band formation. Comparisons of the stress-strain-strength response of cubical, pure shear, plane strain (PS), and simple shear specimens to axisymmetric, isotropically consolidated triaxial compression tests indicate that the strength and stiffness of this well-graded soil in plane strain are larger than expected. Additional comparisons to three-dimensional failure criteria that incorporate the intermediate principal stress are made and show that the Matsuoka-Nakai failure criterion underestimates the strength, but that the Lade-Duncan failure criterion sufficiently estimates the strength of Kanaskat gravel. The stress-dilatancy response of Kanaskat gravel is compared to Bolton's (1986, 1987) empirical relationships and shows that some, but not all, simple expressions may be used to estimate the dilatancy of a well-graded granular soil.

Experimental Program

The relative density selected for the tests in this study models the compacted reinforced fill within MSE walls that were constructed as part of the SeaTac International Airport (STIA) third runway expansion project described by Stuedlein et al. (2007, 2010, 2012). Sourced from a quarry in Kanaskat, Washington and selected based on specified limits put forth by the designers, the sandy gravel soil characteristics tested in accordance with ASTM (2006, 2009) standards are presented in Table 1. Its gradation, representing an average of six samples from a large stockpile, is presented in Fig. 1 along with the project-specified gradation limits. The roundness and sphericity of Kanaskat gravel was quantified following the procedures for Krumbein and Sloss (1963); based on the classification system proposed by Powers (1953), Kanaskat gravel is characterized as rounded to subrounded. The mineral content of Kanaskat gravel was evaluated using X-ray diffraction, which indicated that the composition primarily consists of quartz with some potassium feldspar and hornblende which have mineral surface friction angles ranging from 22 to 35°, 36 to 38°, and 31°, respectively (Terzaghi et al. 1996).

The research presented in this study focused on the stresses and states representative of tall MSE walls (i.e., fills). As a result, consolidation stresses, presented in Table 2, for the AICD and PSK₀CD tests were selected based on mean effective consolidation pressures, p'_c , representative of conditions in a tall MSE wall, and tests were conducted at the postconsolidation relative density to simulate void ratio changes expected during wall construction. The AICD and PSK₀CD tests were conducted to assess the effects of confining pressure and stress path on the strength and dilation of Kanaskat gravel and to provide a benchmark for interpretation of experiments on the performance of closely spaced reinforcement strips not described here. Mean effective stresses at consolidation for each stress path, presented in Table 2, used for the AICD tests ranged from 10 to 1,000 kPa to study the stress-strain-strength response over a wide range in stresses using a conventional stress path, whereas p'_c

Table 1. Characteristic Soil Properties of Kanaskat Gravel

Parameter	Value
D_{10} (mm)	0.22
D_{50} (mm)	6
C_u	46
C_c	0.4
e_{min}	0.182
e_{max}	0.365
$\gamma_{d,max}$ (kN/m ³)	22.4
w_{opt} (%)	6.4

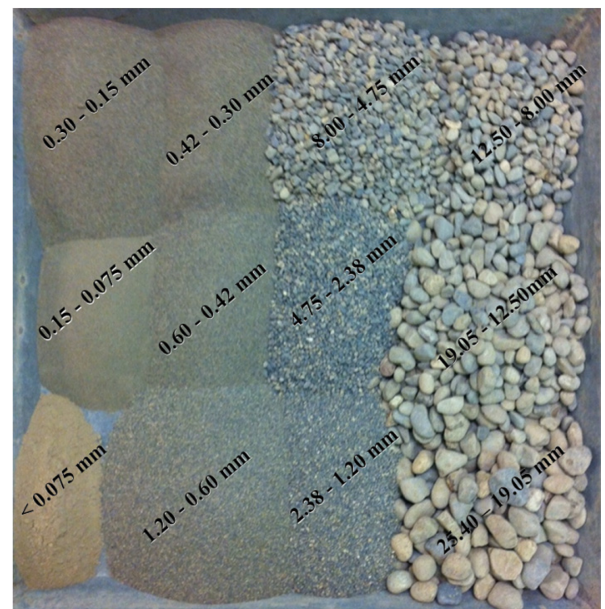
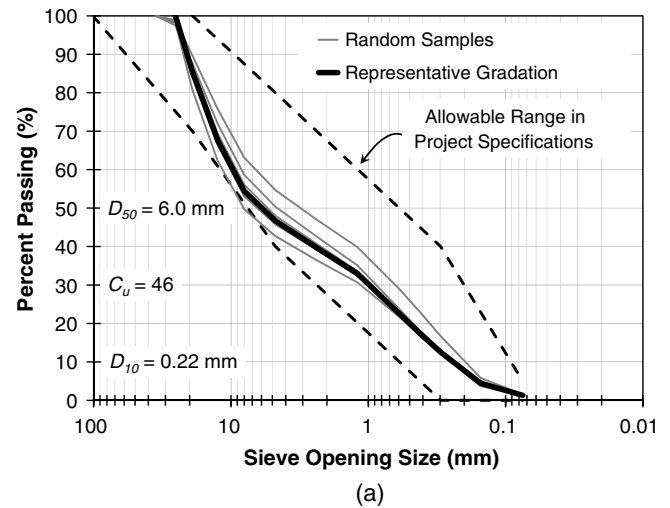


Fig. 1. Grain size distributions of a sandy gravel: (a) sample and representative (target) distributions; (b) example distribution presenting particle shape

ranged from 28 to 172 kPa for the less-common PSK₀CD tests owing to experimental limitations.

Specifications at the STIA third runway project required that the reinforced fill be compacted to 92% of the maximum Modified Proctor (ASTM 2006) dry unit weight, $\gamma_{d,max}$, with corresponding optimum moisture content, w_{opt} , at $\pm 2\%$ (Stuedlein et al. 2010). For Kanaskat gravel, $\gamma_{d,max} = 22.4$ kN/m³ at $w_{opt} = 6.4\%$ as shown in Table 1. In consideration of project specifications, each test specimen was compacted to a target $\gamma_d = 21.3$ kN/m³, corresponding to a relative density of 65%; deviations of $\pm 2.5\%$ in actual relative density were allowed. Details for AICD specimen preparation are described by Walters (2013). Most of the triaxial compression tests were compacted slightly below the target relative density of 65% with the lowest value being 63% and the highest being 66%. Similarly, initial relative densities for the PSK₀CD tests ranged from 64 to 67%. Relative density changes that occur during consolidation are presented in Fig. 2 as a function of p'_c normalized by a reference pressure, $p_{ref} = 101.3$ kPa, which shows that

Table 2. Overview of the Laboratory Testing Program and Relevant Results

Stress path	Mean effective consolidation stress [p'_c (kPa)]	Significant void ratios ^a				Friction angle at failure [ϕ'_f (°)]	Dilation angle at failure [ψ_f (°)]
		e_{bc}	e_{ac}	e_f	e_{cs}		
AICD	10	0.250	0.249	0.256	0.276	54.1	22.6
	20	0.248	0.246	0.253	0.275	51.5	18.7
	50	0.248	0.242	0.248	0.264	48.7	14.7
	100	0.250	0.241	0.247	0.260	45.2	11.2
	250	0.248	0.231	0.235	0.245	43.6	8.7
	500	0.248	0.231	0.228	0.235	42.9	4.2
	1,000	0.246	0.227	0.222	0.227	41.6	2.0
PSK ₀ CD	28	0.246	0.246	0.251	N/A	64.6	—
	63	0.243	0.242	0.246	N/A	65.4	30.4
	86	0.244	0.240	0.247	N/A	62.5	27.9
	114	0.245	0.237	0.246	N/A	62.6	27.2
	142	0.247	0.237	0.245	N/A	56.8	25.1
	172	0.242	0.234	0.242	N/A	57.0	23.0

Note: AICD = axisymmetrical isotropically consolidated drained; PSK₀CD = plane strain quasi- K_0 consolidated drained.

^a bc = before consolidation, ac = after consolidation, f = at failure, and cs = critical state.

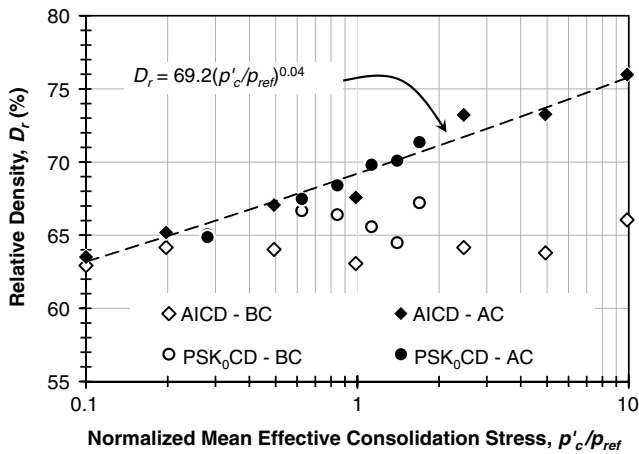


Fig. 2. Changes in relative density due to consolidation as a function of confining pressure for axisymmetrical isotropically consolidated drained (AICD) and plane strain quasi- K_0 consolidation drained (PSK₀CD) tests on Kanaskat gravel; AC = after consolidation, BC = before consolidation

although the sample was initially compacted to $D_r \approx 65\%$, D_r as high as 76% were observed before the onset of shearing.

Axisymmetric Isotropically-Consolidated Drained Response

Seven cylindrical AICD specimens (diameter = 152 mm, height = 305 mm) were sheared at 0.05%/min to provide a baseline stress-strain-strength and volumetric response of Kanaskat gravel for comparison to the plane strain stress path. In order to directly compare results of different stress paths, intermediate principal stresses were incorporated by adopting the three-dimensional form of the deviatoric stress, q , which is given by

$$q = \sqrt{3J_2} \quad (3)$$

where J_2 = second stress invariant. Similarly, the mean effective stress, p' , defined as

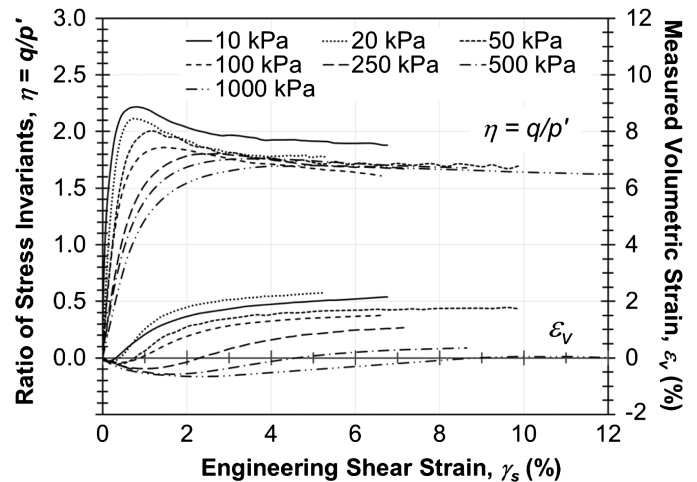


Fig. 3. Stress invariant ratio and volumetric strain response of Kanaskat gravel developed from AICD triaxial tests

$$p' = \frac{(\sigma'_1 + \sigma'_2 + \sigma'_3)}{3} \quad (4)$$

was adopted, where σ'_1 , σ'_2 , and σ'_3 = major, intermediate, and minor principal effective stress, respectively. Fig. 3 presents the AICD responses of specimens in terms of the stress invariant ratio, $\eta = q/p'$, as a function of engineering shear strain, γ_s , calculated using the three-dimensional form given by

$$\gamma_s = \sqrt{\frac{4}{3}J_2''} \quad (5)$$

where J_2'' = second invariant of the deviatoric strain tensor. Generally, increases in confining stress results in reductions in peak η , increases in shear strain to failure, and the suppression of dilation.

Fig. 4 presents AICD friction and dilation angles at failure, $\phi'_{f,AICD}$ and $\psi_{f,AICD}$, respectively, where failure in the AICD stress path is defined at the peak stress invariant ratio. The AICD friction angles at failure range from 54 to 42° and were corrected for the geostatic stress gradient in the sample by adding the average (i.e., midpoint) geostatic vertical stress, approximately 7 kPa to the major principal stress, σ'_1 . The largest change in the friction angle as

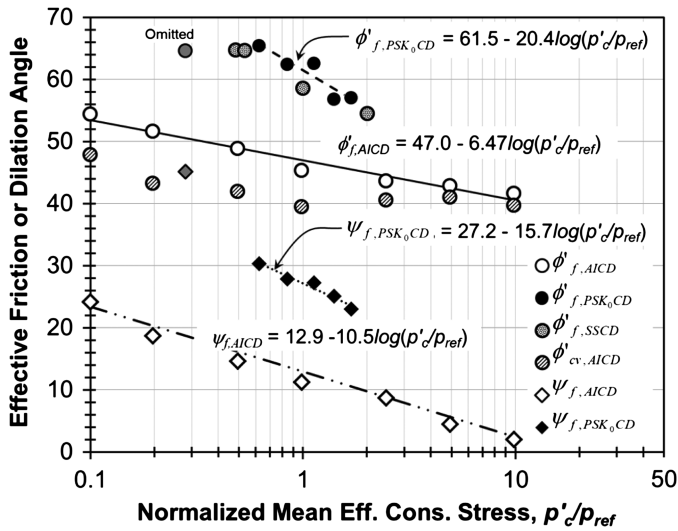


Fig. 4. Effective friction and dilation angles at failure as a function normalized mean effective stress for AICD and PSK₀CD tests; shaded points were removed from the PSK₀CD trends due to boundary condition effects at low confining stresses

a result of the pressure gradient in the sample was approximately 1° at the lowest confining pressure test. The friction angles are fitted using a log-linear relationship and deviations from this trend correspond to differences between the initial relative densities of specimens. The corresponding dilation angles for the AICD tests ranged from 2 to 23° as presented in Fig. 4.

Void ratio paths, presented in Fig. 5, indicate the change in the global void ratio during shearing in the AICD and PSK₀CD stress paths. Markers in Fig. 5 indicate the void ratio at consolidation, e_c , at failure, e_f , and at the critical state, e_{cs} . The observed void ratio paths during shearing in the AICD stress path show that all specimens initially contracted and then expanded towards the critical state with significant changes in p' . Conversely, no contraction was observed in the void ratio path in the PSK₀CD stress path, indicating that the specimen dilated until failure with only slight increases in p' . Owing to its fundamental correlation to geotechnical performance measures (Been and Jefferies 1985), it is of interest to understand the evolution of the state parameter, $\Psi = e - e_{cs}$, of Kanaskat gravel during shear. However, this can only be observed for the AICD specimens due to the inability to observe the critical state response in the PSK₀CD tests, as discussed subsequently. Fig. 6 provides state paths for the AICD specimens during shearing, with markers showing the state parameter at consolidation, Ψ_c , and at failure, Ψ_f , and where negative state parameters indicate a dense state. Owing to its well-graded nature, the change in void ratio required to achieve the critical state is much smaller than that observed for uniform sands (e.g., Been and Jefferies 1985; Been et al. 1991) over the same range in p'_c . The state paths indicate that the magnitude of contraction is much greater at higher confining pressures, and that Kanaskat gravel begins and ends shearing at the critical state for $p'_c = 1$ MPa and post-consolidation $D_r = 76\%$.

Tests in the AICD stress path were sheared to different quantities of strain and some of them may not have reached a true critical state. However, comparison of trends presented Figs. 5 and 6 suggests that all tests were sheared sufficiently to reach a representative constant volume state and further shearing would not have changed the results significantly. As a result, the observed stress-strain response at larger strains and void ratio evolution was used to estimate the constant volume or critical state of the soil. Constant

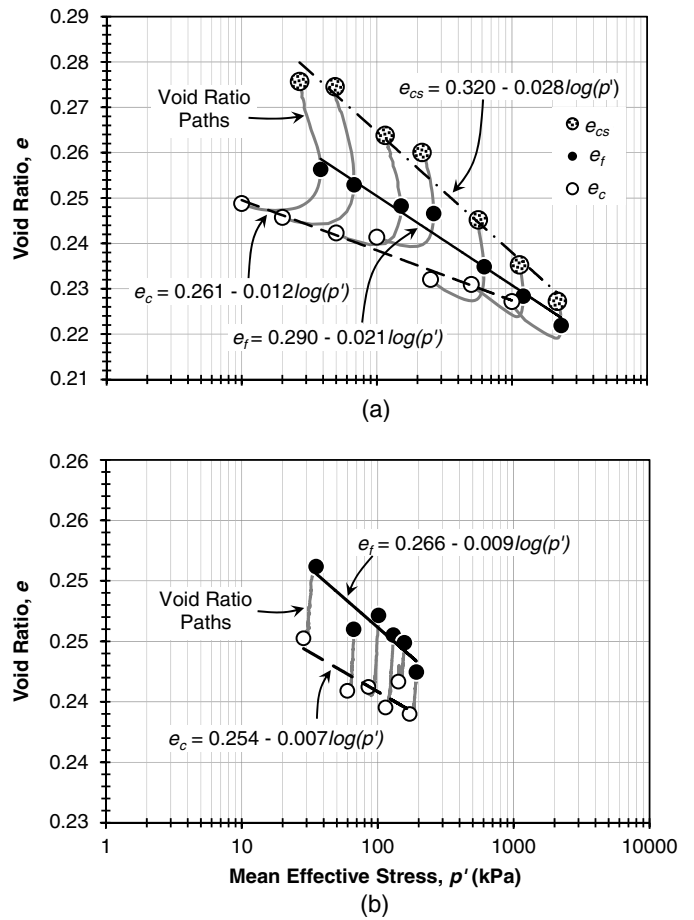


Fig. 5. Evolution of void ratios during shear for (a) AICD; (b) PSK₀CD tests on Kanaskat gravel; e_c , e_f , and e_{cs} correspond to the void ratio at consolidation, failure, and the critical state, respectively

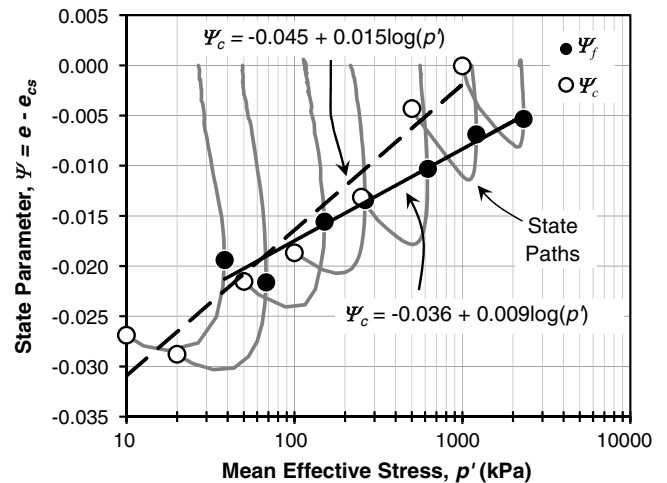


Fig. 6. State paths during shearing of the AICD stress path tests as a function of mean effective stress with indicators showing the state parameters following consolidation and at failure; data for $p'_c = 10$ kPa omitted

volume friction angles (quantified at the end of each test), ϕ'_{cv} , presented in Fig. 4 appear to reduce slightly with increases in confining pressure. An average ϕ'_{cv} of 40° is consistent with a 41° constant volume friction angle reported by Zhao et al. (2013) for a

gravely sand with roughly similar gradation characteristics ($D_{50} = 3.0$ mm, $D_{max} = 10$ mm, and $C_u = 14.3$) tested in a triaxial compression stress path at low confining pressures.

Quasi- K_0 Consolidated Pure Shear Plane Strain Response

The cubical true triaxial apparatus (TTA) described by Hoopes (2007), Choi et al. (2008), and Biggerstaff (2010) allowed testing of Kanaskat gravel due to its internal dimensions, equal to 240 mm in each direction. The stress-controlled TTA is able to measure the intermediate principal stress using load cells, but is unable to capture softening responses due to its use of flexible membranes (Arthur 1988; Choi et al. 2008). Hence, the deviatoric stress-strain and volumetric strain response deviates from that observed in the AICD test series. Additionally, the geometry and boundary conditions of the TTA alters the development of shear bands and strain compatibility during shearing. This results in the development of a quasi- K_0 consolidation mechanism that impacts the stress-strain and volumetric responses of Kanaskat gravel. Efforts to interpret the response of Kanaskat gravel with regard to these experimental conditions are explained in subsequent subsections.

Quasi- K_0 Consolidation Behavior

True K_0 consolidation requires one-dimensional strain (Terzaghi et al. 1996); consolidation of specimens in the TTA and similar devices (Wanowski and Chu 2008) results in strains in both the σ'_1 and σ'_2 directions and produces a quasi- K_0 consolidation stress path. Consolidation in the TTA device was accomplished by applying an increase in σ'_1 and σ'_2 while applying a constant minor principal effective stress equal to the backpressure. This was done to prevent the rubber membrane and specimen from separating from the load cells and influencing control of σ'_3 . The resulting stress path during consolidation, presented in Figs. 7 and 8, produced shear stresses in the specimen prior to failure and as a result, slight differences in the compaction protocol, boundary conditions, and relative density likely affected the consolidation stress path. For example, the shallowest consolidation line (corresponding to $p'_c = 172$ kPa) is indicative of a slightly higher D_r . Additionally, compressive strains on the order of 0.05% in the σ'_3 direction occurred due to compliance associated with strains in the intermediate load

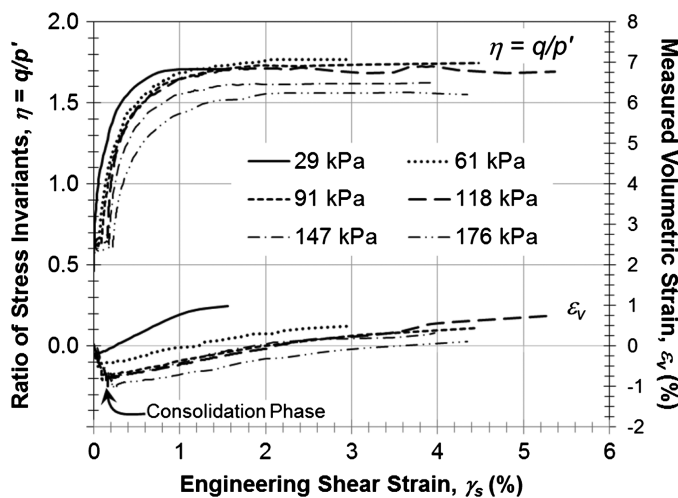


Fig. 7. Ratio of stress invariants and volumetric strain as function of engineering shear strain for the PSK₀CD stress paths

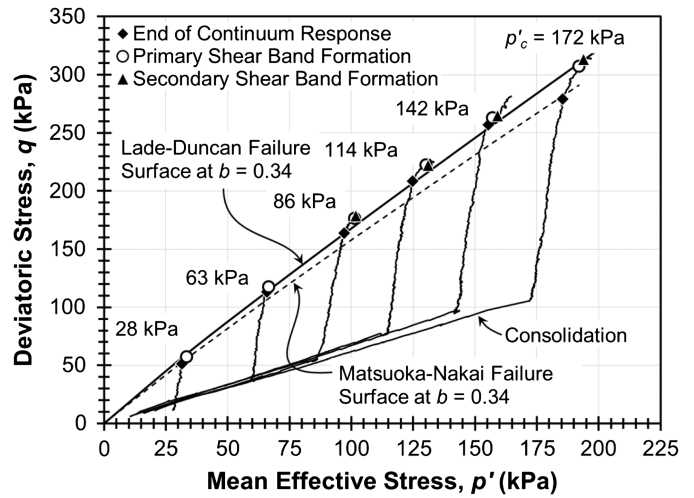


Fig. 8. PSK₀CD stress paths of a sandy gravel in q - p' space with markers indicating the formation of shear bands and deviations from continuum response

cells, which produce a non-zero intermediate strain, ϵ_2 , during consolidation. However, results from PS tests performed by Marachi et al. (1981) indicate that small magnitudes of ϵ_2 do not appreciably affect the plane strain behavior of soil; therefore, ϵ_2 was not considered to affect the strength of specimens presented herein.

The deviatoric stress and volumetric strain response of the PSK₀CD test specimens are shown in Fig. 9. Fig. 9(a) shows that the specimens did not exhibit strain softening following failure, in marked contrast to the AICD test specimens, owing to the stress-controlled test protocol. The plotted deviatoric response includes shearing incurred during consolidation. The volumetric response of Kanaskat gravel in the TTA was independently measured using both linear voltage displacement transducers (LVDTs) centered behind the rubber bladders and a burette with a differential pressure transducer. The LVDTs were used to calculate shear strains from the principal displacement of a cubical soil element. However, volumetric burette readings more accurately represent the response of the entire sample and were used to estimate the average volumetric response. Two assessments of volumetric strain, presented in Figs. 9(b and c), were made: those that were calculated using the trace of the principal strain vector as described by Choi et al. (2008) and those measured using the burette. Choi et al. (2008) showed that the bladder deformation pattern in the TTA was fairly uniform, even at higher displacements, for tests on uniform granular soils and in the absence of shear bands. Fig. 9 indicates that the calculated volumetric strains [Fig. 9(b)] deviate significantly from the measured volumetric strains [Fig. 9(c)] as shearing progresses. Owing to the potential development of shear bands in specimens of Kanaskat gravel, the assessment of dilatancy required careful interpretation of the volumetric and principal strains, as described further in the following sections.

Stiffness of Kanaskat Gravel

The stiffness of the AICD and PSK₀CD tests on Kanaskat gravel may be represented using a secant shear modulus, G , presented in Fig. 10 as a function of p'_c/p_{ref} . The secant shear modulus in the AICD stress path, G_{AICD} , was calculated at a postconsolidation shear strain of 0.05% assuming that the volumetric and shear strains were decoupled; for this case, $G_{AICD} = \Delta q / (3\Delta\gamma_s)$ where Δq is the change in deviatoric stress and $\Delta\gamma_s$ is the change in the shear

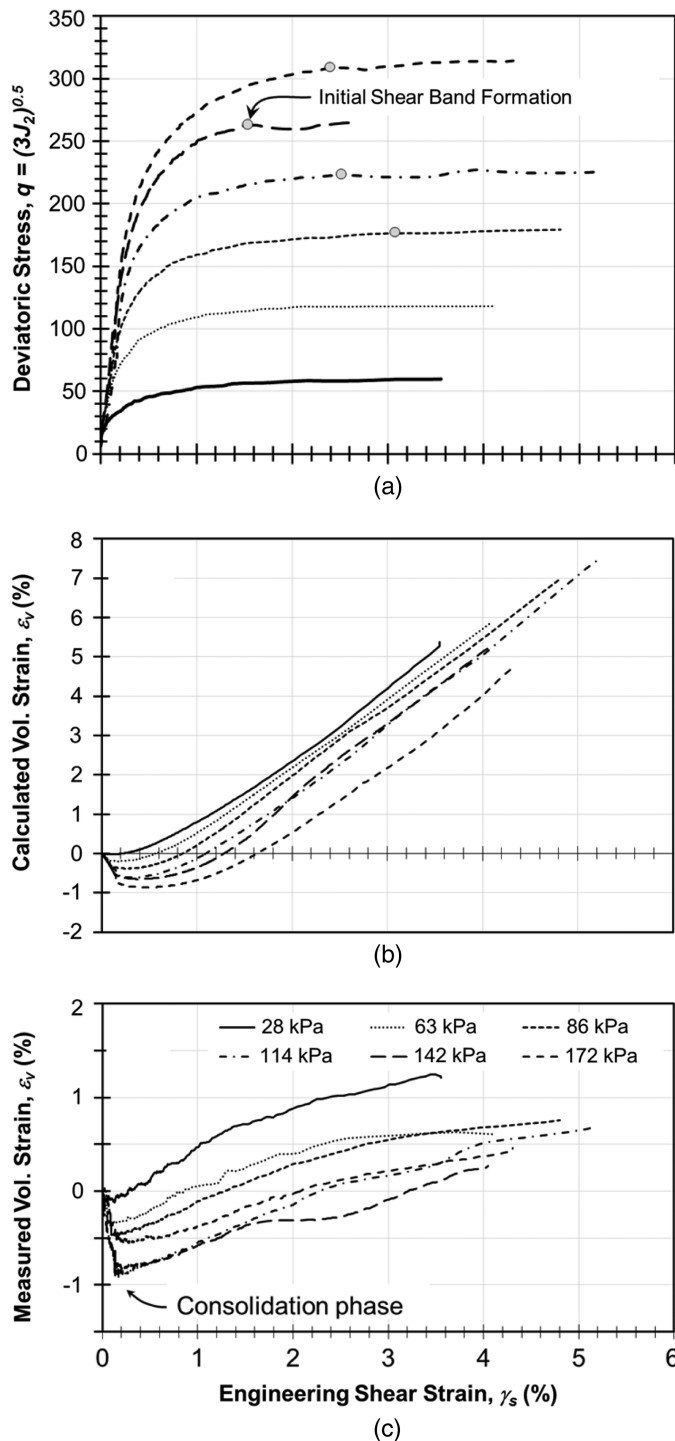


Fig. 9. PSK₀CD specimen response during consolidation and shearing: (a) deviatoric stress-strain response; (b) volumetric strain calculated using LVDTs in principal directions; (c) volumetric strain measured using burette observations

strain (Wood 1990). The computed G_{AICD} ranged between 9 MPa at a p'_c of 10 kPa and 70 MPa at a p'_c of 1 MPa. The fitted power law exponent, equal to 0.56, is consistent with those reported in the literature (Schanz and Vermeer 1998). The initial tangent shear modulus corresponding to the PSK₀CD stress path, G_{PSK0CD} , was calculated at a postconsolidation shear strain of 0.05% and in consideration of the pure shear stress path (i.e., constant mean effective stress). Therefore $G_{PSK0CD} = \Delta q / \Delta \gamma_s$. At a given p'_c , the calculated

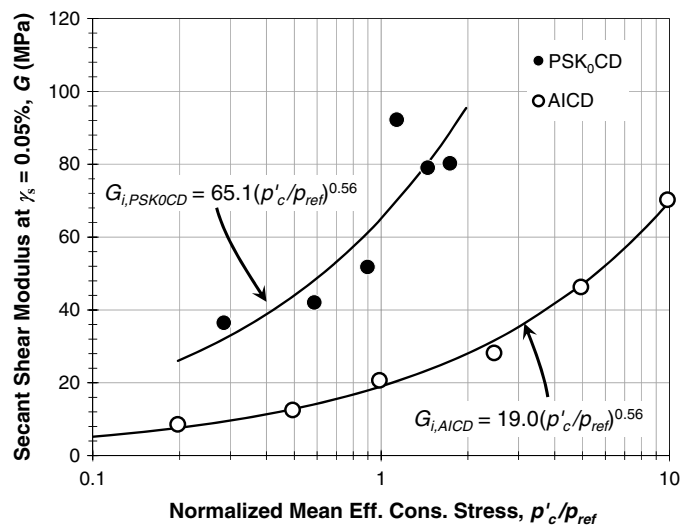


Fig. 10. Initial tangent shear modulus computed at 0.05% shear strain and plotted versus p'_c/p_{ref}

shear modulus for PSK₀CD specimens were significantly greater than those of the AICD specimens, and ranged from 37 to 92 MPa for p'_c of 28 to 172 kPa. The increase in the shear modulus in the PSK₀CD stress path is attributed to the increase in p' stemming from the greater σ'_2 (Hatami and Bathurst 2005). As a result, the power law describing the G_{PSK0CD} data is characterized with a significantly larger fitted coefficient; however, a similar power law exponent (i.e., 0.52) was back-calculated from the observed PSK₀CD test data. A power law with an exponent equal to 0.56 is plotted in Fig. 10, as it should theoretically be material-specific and independent of stress path (the power law is relatively insensitive to the difference in these two exponents over the stress range considered).

Strain Compatibility and Shear Band Formation

The predominant failure mechanism in typical prismatic PS tests (i.e., with aspect ratios of 2:1) is the formation of a single well-defined shear band (e.g., Lee 1970; Evans and Frost 2010), typically evident by strain softening. The stress-controlled protocol required by the TTA did not allow for the observation of constant volume behavior, resulting in PSK₀CD responses [Figs. 7 and 9(a)] that do not reduce to a critical state like AICD specimens (Fig. 3). However, the measured volumetric and principal displacement measurements and fluctuations in the deviatoric response provided indications that shear bands formed during shear. The calculated volumetric strain [Fig. 9(b)] initially follows the measured volumetric response but deviates significantly after about 1% shear strain, which suggests that the specimen transitions from a continuum to bifurcation response (Bardet 1991). After bifurcation, the measured volumetric response of the soil is primarily dependent on the soil in the shearing zone, which has essentially reached a constant volume state. Shear banding of cubical specimens is evident in Fig. 9(b) for those portions of the measured volumetric strain measurements that exhibit shear strains with little to no change in volumetric strain. The test conducted at $p'_c = 142$ kPa exhibits the most-apparent development of a shear band, occurring at approximately $\gamma_s = 1.7\%$. The formation of shear bands within cubical specimens impacted the deformations observed at the flexible bladders, resulting in the inability to adequately measure rigid block sliding during bifurcation.

Fig. 11 presents the principal displacement measurements, δ , for a PSK₀CD test at a $p'_c = 114$ kPa as a function of γ_s .

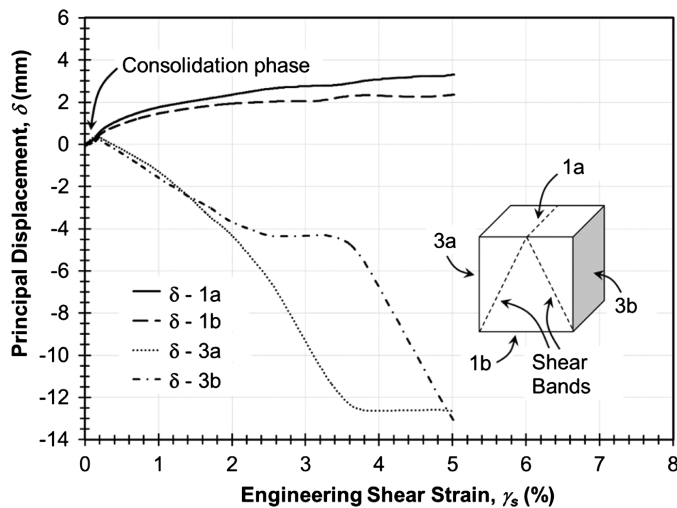


Fig. 11. Progression of principal displacements for $p'_c = 114$ kPa; inset shows major principal (i.e., Faces 1a and 1b) and minor principal faces (Faces 3a and 3b) showing hypothetical shear band locations

The displacements in the major principal directions are positive, indicating compression, whereas displacements in the minor principal direction are negative and indicate extension. Significant deviations between measurements in the minor principal direction are observed at approximately $\gamma_s = 1.75\%$, indicating that Face 3a begins translating whereas Face 3b ceases to displace. At approximately $\gamma_s = 3.5\%$, the behavior reverses and Face 3a stops and Face 3b starts to displace, suggesting that the cubical sample developed two shear bands. Shapiro and Yamamuro (2003), Abelev and Lade (2003), and Lade and Abelev (2003) showed that at least two shear bands can develop in cubical devices as a result of the geometrical constraints of the device that intersect the top or bottom of a cubical specimen without significantly altering the measured peak friction angles. Considering the geometry of the TTA, shear bands can hypothetically daylight at the center of the top or bottom (i.e., major) faces of the cube as shown in Fig. 11 inset. However, due to limitations of the testing device, no methods were used to obtain the actual angle of inclination of the specimens; therefore, the schematic in Fig. 11 represents an estimated or hypothetical geometry.

The measured change in specimen volume is therefore associated with shearing along these zones and the corresponding dilation angle can be approximated using Eq. (2) and the measured volumetric response just prior to the onset of initial shear banding. The resulting ψ_{f,PSK_0CD} presented in Fig. 4 are on average 2.2 times greater than $\psi_{f,AICD}$ and reduce from 30 to 23° over the range of confining stresses investigated. Although large, the measured PSK₀CD dilation angles are similar in magnitude to those resulting from cubical true triaxial tests on Santa Monica beach sand at effective confining stresses of 50 kPa reported by Lade and Abelev (2003). Lade and Abelev (2003) showed that dilation angles of uniform sands in the plane strain stress path can be on the order of 70% larger than those measured in triaxial compression. Here, the observed PSK₀CD dilation angles on well-graded sandy gravel are approximately 100% larger than those resulting from the AICD stress path.

Effect of Intermediate Stresses and Strains

Fig. 8 presents the PSK₀CD stress path to failure and describes key milestones in specimen response during shearing. The

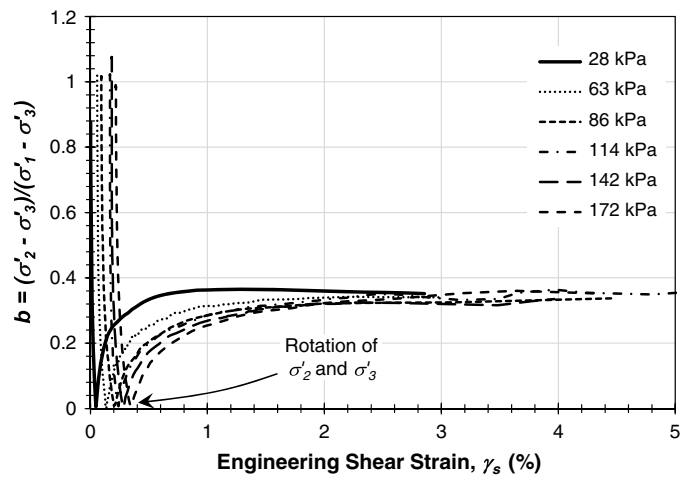


Fig. 12. Progression of the intermediate deviatoric stress ratio during shearing in the PSK₀CD stress path

end-of-continuum response was defined by the onset of deviation in the principal displacements along the minor principal directions (Fig. 11), and corresponded to the initiation of shear banding. During shearing, σ'_1 and σ'_2 were uniformly increased and decreased at 1.5 kPa/min, respectively, to produce an applied near-constant p' stress path. As shown in Fig. 8, a constant p' stress path was not achieved during shear, owing to increases in stresses in the restrained direction.

The intermediate differential stress ratio, b , is used to define the stress state in relation to triaxial compression (TC) and extension (TE) stress paths, where

$$b = \frac{\sigma'_2 - \sigma'_3}{\sigma'_1 - \sigma'_3} \quad (6)$$

The magnitude of b is stress path-dependent and bounded between 0 (i.e., TC) and 1 (i.e., TE), respectively. Green (1971), Reades and Green (1976), Tatsuoka et al. (1986), and Peters et al. (1988) have shown that the strength of soil in plane strain ($b \approx 0.3$) or other intermediate stress states is larger than that for triaxial compression stress paths. On average, PSK₀CD specimens of Kanaskat gravel at failure exhibited $b = 0.34$, similar to the typical range of 0.2 to 0.4, depending on sample density, anisotropy, and testing device, for PS specimens (e.g., Green 1971; Reades and Green 1976; Peters et al. 1988). Failure was defined as the stress invariant ratio that corresponds to the formation of the initial shear band.

Fig. 12 presents the progression of b during shearing for the PSK₀CD test specimens. Initially, b is approximately equal to 1 as a result of the quasi- K_0 consolidation stress path. Upon initiation of shear, b drops rapidly to 0, indicating the rotation of the minor principal stresses, whereupon the restrained direction becomes σ'_2 . Fig. 13 presents the evolution of stresses measured in the restrained direction during consolidation and shearing; markers indicate the initiation of shear (i.e., end-of-consolidation) and the rotation of σ'_2 and σ'_3 . During consolidation, σ'_2 increases in a near-linear manner with increases in p'_c . However, during shearing, σ'_2 decreases while σ'_3 increases until these principal stresses rotate, after which the restrained direction serves to host the intermediate principal effective stress. Thereafter, σ'_2 increases with rapid straining to failure and subsequent increases in the mean effective stress, producing the stress path presented in Fig. 8. Phusing et al. (2015) conducted true-triaxial DEM simulations with varying and constant b to determine that the shape and location of the yield surface is independent of the

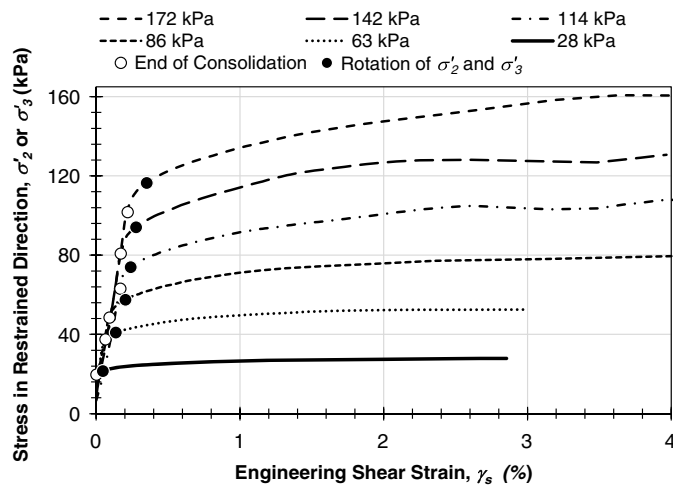


Fig. 13. Development of intermediate principal stresses for the PSK₀CD consolidation and shearing stress paths

stress path, and therefore, the yield surface identified herein is considered insensitive to the selected stress path.

Fig. 4 presents the PSK₀CD friction angles at failure for Kanaskat gravel, which are computed by finding the intersection of the three-dimensional stress path with the Mohr Coulomb (M-C) failure criterion

$$\phi' = \sin^{-1} \left[\frac{\frac{q}{\sqrt{3}} \sin(\theta_L + \frac{1}{3}\pi)}{p' + \frac{q}{\sqrt{3}} \cos(\theta_L + \frac{1}{3}\pi)} \right] \quad (7)$$

where θ_L = lode angle, defined as the angle between the failure point on the three-dimensional surface and the major principal stress direction. The lode angle is related to b by (Suzuki and Yanagisawa 2006)

$$\theta_L = \tan^{-1} \left(\frac{\sqrt{3}b}{2-b} \right) \quad (8)$$

The log-linear trend shown in Fig. 4 did not include the PSK₀CD test at $p'_c = 28$ kPa due to the exaggerated boundary condition effects associated with the flexible membranes at such low confining pressures.

Friction angles for Kanaskat gravel in plane strain, presented in Fig. 4, have been corrected for geostatic stresses (i.e., 5 kPa) similar to the AICD tests and are approximately 33% larger than those resulting from AICD stress paths. This is larger than that expected given the typical magnitudes reported for plane strain (Jewell and Wroth 1987; Kulhawy and Mayne 1990), which are generally 20–10% larger than in triaxial compression. However, typical ranges were developed on the experimental basis of uniformly graded soils with lower AICD friction angles. Koerner (1970) and Mitchell and Soga (2005) suggest that greater shear resistance in well-graded soils is associated with a greater degree of fabric anisotropy, the presence of larger particles in the soil matrix, and lower void ratios which produce a greater number of frictional contacts. As a result, the measured frictional responses of well-graded materials will be subject to the influence of stress path effects, relative density, and changes in p' that are not readily apparent in Fig. 7. The large magnitude of the measured friction angles prompted additional cubical triaxial testing to verify the measured plane strain response. Friction angles measured for the simple shear consolidated drained (SSCD) stress path tests on Kanaskat gravel

using the TTA are shown in Fig. 4. The σ'_2 was not allowed to change in the SSCD tests; thus, compared to the PSK₀CD friction angles, the SSCD friction angles are slightly smaller. However, they are of similar magnitude and trend as the plane strain friction angles.

Comparisons between measured PSK₀CD responses, and calibrated three-dimensional failure criteria can be used to assess the validity of the larger peak response in consideration of σ'_2 . The Matsuoka-Nakai (M-N) or Lade-Duncan (L-D) criteria (Matsuoka et al. 1974; Lade and Duncan 1973), presented in Fig. 8 indicate that the increase in peak strength can be sufficiently predicted by well-established three-dimensional failure criteria. The M-N failure surface calibrated to the AICD data is presented in Fig. 8 at $b = 0.34$. The plotted M-N failure criterion fitting parameter, ξ , was best represented using bilinear functions of p'_c normalized by p_{ref}

$$\xi = 0.96 \left(\frac{p'_c}{p_{ref}} \right)^{-0.134} \quad \text{for } \frac{p'_c}{p_{ref}} < 1;$$

$$\xi = 0.96 \left(\frac{p'_c}{p_{ref}} \right)^{-0.059} \quad \text{for } \frac{p'_c}{p_{ref}} \geq 1 \quad (9)$$

and produced lower deviatoric stresses at a given mean effective stress than those measured. However, the observed curvature of the trend is similar to the fitted trend. The L-D failure criterion requires the fitting of coefficient κ , which was calibrated to the TC stress path using the AICD data and was also best-represented using bilinear functions of p'_c/p_{ref} for Kanaskat gravel

$$\kappa = 83.8 \left(\frac{p'_c}{p_{ref}} \right)^{-0.278} \quad \text{for } \frac{p'_c}{p_{ref}} < 1;$$

$$\kappa = 84.0 \left(\frac{p'_c}{p_{ref}} \right)^{-0.095} \quad \text{for } \frac{p'_c}{p_{ref}} \geq 1 \quad (10)$$

The L-D failure criterion satisfactorily estimates the deviatoric stress of PSK₀CD specimens at failure. The PSK₀CD strength predicted using the L-D failure criterion fitted to the AICD specimens, in concert with comparison to SSCD friction angles, suggests that the observed PSK₀CD friction angles appropriately represent the highly frictional behavior of Kanaskat gravel in plane strain.

Discussion of the Stress-Dilatancy Behavior of Kanaskat Gravel

Bolton (1986) proposed an empirical approach to Rowe's (1962, 1969) and Rowe et al.'s (1964) stress-dilatancy theory using a database of 17 uniform sands to capture the effect of the rate of dilation, relative density, and mean effective stress with the relative dilatancy index, I_R

$$I_R = D_R \left[Q - \ln \left(\frac{p'_f}{p_{refB}} \right) \right] - R \quad (11)$$

where p_{refB} = reference pressure typically equal to 1 kPa; D_r = relative density in decimal form; and Q and R = fitting coefficients equal to 10 and 1, respectively. The statistical regression for the dilatation component of strength was found equal to

$$\phi'_f - \phi'_{cv} = A_{\psi,PS} I_R = A_{\psi,TC} I_R \quad (12)$$

where $\phi'_f - \phi'_{cv}$ = measure of dilatancy; $A_{\psi,PS} = 5$; $A_{\psi,TC} = 3$; and the subscripts PS and TC = plane strain and triaxial compression, respectively. In a response to Tatsuoka (1987), Bolton (1987) presented data on uniform Toyoura sand to show that Eq. (11)

over-predicts $\phi'_f - \phi'_{cv}$ at low mean effective stresses ($p' < 150$ kPa). Bolton (1987) attributed the resulting error to an apparent increase in ϕ'_{cv} at low to very low σ'_3 , and proposed improved empirical correlations as a function of p' . More recently, Salgado et al. (2000) and Chakraborty and Salgado (2010) confirmed that Bolton's Q decreases with a decrease in σ'_3 below approximately 200 kPa for Toyoura Sand, which was also attributed to changes in ϕ'_{cv} .

Eq. (11) is a formulation of Eq. (1) in which the a coefficient was empirically derived by Bolton (1986) to be equal to 0.8 in plane strain and 0.48 in triaxial compression. Fig. 14(a) presents the variation of $\phi'_{f,AICD}$ and ϕ'_{f,PSK_0CD} with ψ_f along with estimates provided by Eq. (11). The fitted linear trends presented in Fig. 14(a) were established by assuming that ϕ'_{cv} was equal to a constant 40° in the PSK₀CD and AICD stress paths. The resulting fitting coefficient a for use with Eq. (1) is equal to 0.79 and 0.58 for Kanaskat gravel in PSK₀CD and AICD stress paths, respectively.

Fig. 14(b) compares measured $\phi'_f - \phi'_{cv}$ as a function of p'_c/p_{ref} to that approximated by Bolton's (1986) original and modified (Bolton 1987) empirical expressions. Individually measured $\phi'_{cv,AICD}$ were used to compute the $\phi'_f - \phi'_{cv}$ values for the AICD stress path shown in Fig. 14. The effective constant volume friction angle for

the PSK₀CD specimens could not be observed, as described previously (refer to Fig. 9). However, experimental work by Lee (1970) suggests that ϕ'_{cv} is equivalent for plane strain and triaxial compression at high confining pressures. Therefore, the average PSK₀CD constant volume friction angle equal to 40° was used in order to calculate $\phi'_f - \phi'_{cv}$ for the PSK₀CD stress path, based on measured $\phi'_{cv,AICD}$.

Although some differences are noted, there is relatively good agreement between the observed and predicted response of Bolton's (1986) original triaxial compression stress path approximation. However, Bolton's (1987) modified approximation does not adequately capture the trend in $\phi'_f - \phi'_{cv}$ for Kanaskat gravel at low mean effective pressures and for the AICD specimens. This response is attributed to the presence of stronger particles and the larger number of particle contacts in the well-graded soil matrix that dominate the frictional characteristics at lower pressures. Differences in the trends of the measured and predicted PSK₀CD data indicated that Bolton's (1986) approximation of plane strain strength at failure provides a good first approximation. Additionally, the trends suggests that the strength of well-graded sandy gravel is more sensitive to intermediate principal effective stresses than estimated by Bolton's original approximation. Thus, it appears that Bolton's (1986) approximation of Rowe's stress-dilatancy theory may be used to estimate the stress-dilation response of well-graded gravelly soils in both TC and PS stress paths. This suggests that Bolton's fitting coefficients, calibrated to a database of uniform sands, is sufficient for use with well-graded sand and gravel mixtures in practice.

Summary and Conclusion

Geotechnical engineers often use stress-dilatancy theories and approximations that are developed based on uniform sands; however, very little information of this kind exists for well-graded gravelly soils. Pertinent questions regarding the stiffness, strength, and volumetric response of these soils in plane strain remain to be answered. To reduce the evident gap in information, an experimental program was conducted to study the stiffness, strength, and stress-dilatancy of well-graded Kanaskat gravel using axisymmetric, isotropically consolidated drained (AICD) triaxial and cubical pure shear quasi- K_0 consolidated drained (PSK₀CD) plane strain tests over a wide range of confining stresses. Results from the testing program indicate that the stress-dilatancy behavior of Kanaskat gravel differs from that of uniform sands. However the theories developed based on uniform soils can be used to satisfactorily estimate the soil response under typical working stresses.

The secant shear stiffness of PSK₀CD specimens was approximately three times larger than AICD specimens, which indicates that the intermediate strain response has a significant effect on the prefailure response of sandy gravel soils. Additionally, the plane strain friction and dilation angles of Kanaskat gravel at failure are significantly greater than for AICD specimens sheared in triaxial compression, on the order of 33 and 120% larger, respectively. The PSK₀CD response at failure was compared to drained consolidated simple shear tests and three-dimensional failure criteria fitted to AICD specimens and that incorporate the effect of the intermediate principal stress. The Matsuoka-Nakai failure criterion was found to underpredict the observed failure envelope, whereas the Lade-Duncan failure criterion was found to adequately predict the measured PSK₀CD response at failure. Geometrical constraints imposed by the cubical triaxial device impacted the measured volumetric response and inhibited free shear band formation. As a result, two incipient shear bands formed in the TTA requiring careful interpretation of volumetric responses for estimation of the dilation

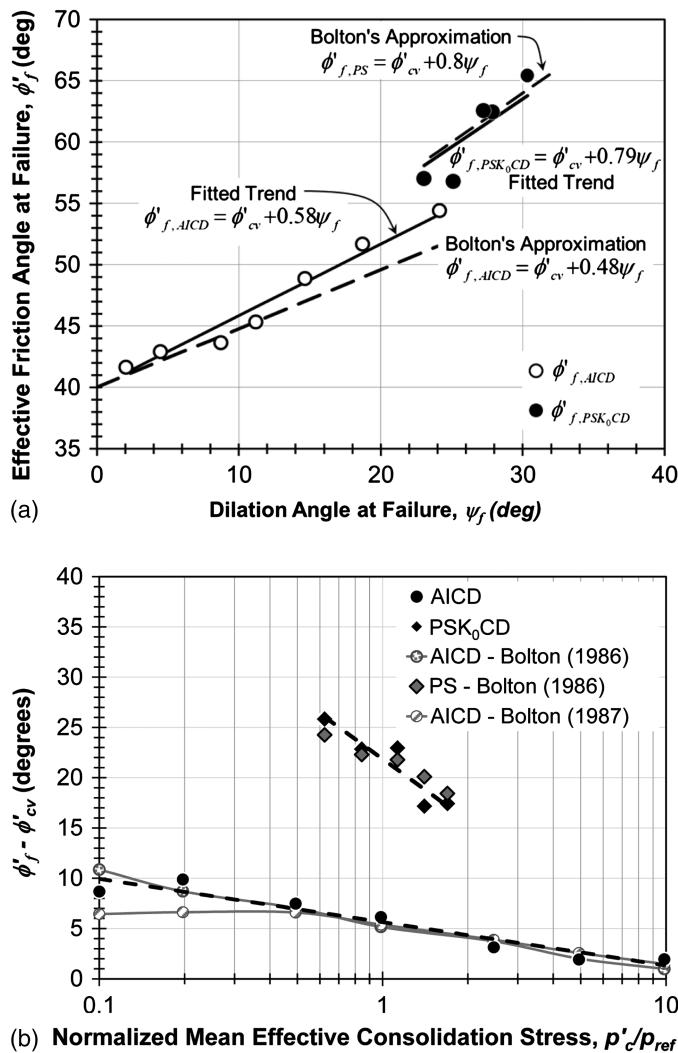


Fig. 14. Stress-dilatancy behavior of Kanaskat gravel: (a) comparison of effective friction and dilation angle at failure; (b) comparison of observations to Bolton's approximation as a function of mean effective confining stress

angle. Comparisons between Bolton's (1986, 1987) approximation of Rowe's (1969) stress-dilatancy theory indicate that in general, the modified approximation does not appear appropriate for low confining stresses. Bolton's (1986) original correlation appeared applicable to the well-graded gravelly soils in the triaxial compression stress path over the range in pressures investigated. The data reported here should help those requiring accurate estimates of the stiffness, strength, and stress-dilatancy of well-graded sandy gravel and improve their confidence in selected design parameters.

Acknowledgments

The material presented herein was supported by the National Science Foundation through Grant Number CMMI 1100903 under Program Director Dr. Richard Fragaszy, and is greatly appreciated. Any opinions, findings, and conclusions expressed in this study are those of the writers and do not necessarily reflect the views of the National Science Foundation. The donation of Kanskat gravel from the Watson Asphalt Paving Company, Inc., of Redmond, Washington is gratefully appreciated. The X-ray diffraction studies were performed with significant support of Dr. John Dilles of Oregon State University. The authors thank Dr. Matthew Evans of Oregon State University for helpful discussions of this work, as well as the anonymous reviewers for their helpful comments and suggestions.

References

- Abelev, A. V., and Lade, P. V. (2003). "Effects of cross-anisotropy on three-dimensional behavior of sand. I: Stress-strain behavior and shear banding." *J. Eng. Mech.*, 10.1061/(ASCE)0733-9399(2003)129:2(160), 160–166.
- Arthur, J. R. F. (1988). "Cubical devices: Versatility and constraints." *Advanced triaxial testing of soil and rock*, R. T. Donaghe, R. C. Chaney, and M. L. Silver, eds., ASTM, Philadelphia, 743–765.
- ASTM. (2006). "Test methods for minimum index density and unit weight of soils and calculation of relative density." *ASTM D4254-06*, West Conshohocken, PA.
- ASTM. (2009). "Test methods for laboratory compaction characteristics of soil using modified effort (56, 000 ft-lbf/ft³ (2, 700 kN-m/m³))." *ASTM D1557-09*, West Conshohocken, PA.
- Bardet, J. P. (1991). "Orientation of shear bands in frictional soils." *J. Eng. Mech.*, 10.1061/(ASCE)0733-9399(1991)117:7(1466), 1466–1485.
- Been, K. and Jefferies, M. G. (1985). "A state parameter for sands." *Geotechnique*, 35(2), 99–112.
- Been, K., Jefferies, M. G., and Hachey, J. (1991). "The critical state of sands." *Geotechnique*, 41(3), 365–381.
- Biggerstaff, D. C. (2010). "Analysis of the effects of the intermediate principal stress on the behavior of gravel with a 9.5 inch true triaxial apparatus." M.S. thesis, Univ. of Washington, Seattle.
- Bolton, M. D. (1986). "The strength and dilatancy of sands." *Geotechnique*, 36(1), 65–78.
- Bolton, M. D. (1987). "Closure of 'The strength and dilatancy of sands' by Tatsuoka, F." *Geotechnique*, 37(2), 219–226.
- Chakraborty, T. and Salgado, R. (2010). "Dilatancy and shear strength of sand at low confining pressures." *J. Geotech. Geoenviron. Eng.*, 10.1061/(ASCE)GT.1943-5606.0000237, 527–532.
- Charles, J. A. and Watts, K. S. (1980). "The influence of confining pressure on the shear strength of compacted rockfill." *Geotechnique*, 30(4), 353–367.
- Choi, C., Arduino, P., and Harney, M. D. (2008). "Development of a true triaxial apparatus for sands and gravels." *Geotech. Test. J.*, 31(1), 1–13.
- Chu, J. (1994). "Study on the stress-dilatancy behavior of sand by strain path testing." *Proc., Pre-Failure Deformation of Geomaterials*, Balkema, Rotterdam, Netherlands, 365–370.
- Cornforth, D. H. (1964). "Some experiments on the influence of strain conditions on the strength of sands." *Geotechnique*, 14(2), 143–167.
- Evans, T. M., and Frost, J. D. (2010). "Multi-scale investigation of shear bands in sand: Physical and numerical experiments." *Int. J. Numer. Anal. Methods Geomech.*, 34(15), 1634–1650.
- Green, G. E. (1971). "Strength and deformation of sand measured in an independent stress control cell." *Proc., Roscoe Memorial Symp. Stress-Strain Behavior of Soils*, G. T. Foulis, London, 285–323.
- Hanna, A. (2001). "Determination of plane-strain shear strength of sand from the results of triaxial tests." *Can. Geotech. J.*, 38(6), 1231–1240.
- Hatami, K., and Bathurst, R. J. (2005). "Development and verification of a numerical model for the analysis of geosynthetic reinforced soil segmental walls under working stress conditions." *Can. Geotech. J.*, 42(4), 1066–1085.
- Holtz, W. G. and Gibbs, J. (1956). "Triaxial shear tests on pervious gravelly soils." *J. Soil Mech. Found. Div.*, 82(1), 1–22.
- Hoopes, O. T. (2007). "Experimental study with a 9.5-in. true-triaxial apparatus: Phase transformation surface mapping and PID strain-control." M.S. thesis, Univ. of Washington, Seattle.
- Houlsby, G. T. (1991). "How the dilatancy of soils affects their behavior." *Proc., 10th European Conf. on Soil Mechanics and Foundation Engineering*, Balkema, Rotterdam, Netherlands, 1189–1202.
- Jewell, R. A., and Wroth, C. P. (1987). "Direct shear tests on reinforced sand." *Geotechnique*, 37(1), 53–68.
- Koerner, R. M. (1970). "Effect of particle characteristics on soil strength." *J. Soil Mech. Found. Eng. Div.*, 96(SM4), 1221–1234.
- Krumbein, W. C. and Sloss, L. L. (1963). *Stratigraphy and sedimentation*, 2nd Ed., Freeman and Company, San Francisco.
- Kulhawy, F. H., and Mayne, P. W. (1990). "Manual on estimating soil properties for foundations." *Final Rep., Project 1493-6, EL-6800*, Electric Power Research Institute, Palo Alto, CA.
- Lade, P. V., and Abelev, A. V. (2003). "Effects of cross anisotropy on three-dimensional behavior of sand. II: Volume change behavior and failure." *J. Eng. Mech.*, 10.1061/(ASCE)0733-9399(2003)129:2(167), 167–174.
- Lade, P. V. and Duncan, J. M. (1973). "Cubical triaxial tests on cohesionless soils." *J. Soil Mech. Found. Div.*, 99(SM10), 793–812.
- Lee, K. L. (1970). "Comparison of plane strain and triaxial tests on sand." *J. Soil Mech. Found. Div.*, 96(SM3), 901–923.
- Lee, K. L. and Seed, H. B. (1967). "Drained strength characteristics of sands." *J. Soil Mech. Found. Div.*, 93(SM6), 117–141.
- Marachi, N., Duncan, J. M., Chan, C. K., and Seed, H. B. (1981). "Plain-strain testing of sand." *Laboratory shear strength of soil*, R. N. Young and F. C. Townsend, eds., ASTM, West Conshohocken, PA, 294–302.
- Marachi, N. D., Chan, C. K., and Seed, H. B. (1972). "Evaluation of properties of rockfill materials." *J. Soil Mech. Found. Div.*, 98(SM1), 95–114.
- Marsal, R. J. (1967). "Large scale testing of rockfill materials." *J. Soil Mech. Found. Div.*, 93(SM2), 27–44.
- Matsuoka, H. and Liu, S. (1998). "Simplified direct shear test on granular materials and its application to rockfill materials." *Soils Found.*, 38(4), 275–284.
- Matsuoka, H., Liu, S., Sun, D., and Nishikata, U. (2001). "Development of a new in situ direct shear test." *Geotech. Test. J.*, 24(1), 92–101.
- Matsuoka, H. and Nakai, T. (1974). "Stress-deformation and strength characteristics of soil under three different principal stresses." *Proc. JSCE*, 232, 59–70.
- Mitchell, J. K., and Soga, K. (2005). *Fundamentals of soil behavior*, Wiley, New York.
- Panda, B. C. and Ghosh, A. K. (2000). "Influence of grain size distribution on dilatancy of sand." *J. Inst. Eng.*, 81(2), 68–70.
- Peters, J. F., Lade, P. V., and Bro, A. (1988). "Shear band formation in triaxial and plane strain tests." *Advanced triaxial testing of soil and rock*, R. T. Donaghe, R. C. Chaney, and M. L. Silver, eds., ASTM, Philadelphia, 604–627.
- Phusing, D., Suzuki, K., and Zaman, M. (2015). "Mechanical behavior of granular materials under continuously varying b values using DEM." *Int. J. Geomech.*, 10.1061/(ASCE)GM.1943-5622.0000506, 04015027.
- Poorooshasb, H. B. and Roscoe, K. H. (1961). "The correlation of the results of shear tests with varying degrees of dilatation." *Proc., 5th Int. Conf. on Soil Mechanics*, Vol. 1, Dunod, Paris, 297–304.
- Powers, M. C. (1953). "A new roundness scale for sedimentary particles." *J. Sediment. Petrol.*, 23(2), 117–119.

- Reades, D. W. and Green, G. E. (1976). "Independent stress control and triaxial extension tests on sand." *Geotechnique*, 26(4), 551–576.
- Reynolds, O. (1885). "The dilating of media composed of rigid particles in contact." *Philosophical Magazine*, Taylor and Francis, London.
- Rowe, P. W. (1962). "The stress-dilatancy relations for static equilibrium of an assembly of particles in contact." *Proc. R. Soc. London, Ser. A*, 269(1339), 500–527.
- Rowe, P. W. (1969). "The relation between the shear strength of sands in triaxial compression, plane strain, and direct shear." *Geotechnique*, 19(1), 75–86.
- Rowe, P. W., Barden, L., and Lee, I. K. (1964). "Energy components during the triaxial cell and direct shear tests." *Geotechnique*, 14(3), 247–261.
- Salgado, R., Bandini, P., and Karim, A. (2000). "Shear strength and stiffness of silty sand." *J. Geotech. Geoenviron. Eng.*, 10.1061/(ASCE)1090-0241(2000)126:5(451), 451–462.
- Schanz, T. and Vermeer, P. A. (1996). "Angles of friction and dilatancy of sand." *Geotechnique*, 46(1), 145–151.
- Schanz, T. and Vermeer, P. A. (1998). "On the stiffness of sands." *Geotechnique*, 48, 383–387.
- Shapiro, S. and Yamamuro, J. A. (2003). "Effects of silt on three-dimensional stress-strain behavior of loose sand." *J. Geotech. Geoenviron. Eng.*, 10.1061/(ASCE)1090-0241(2003)129:1(1), 1–11 .
- Skermer, N. A. and Hillis, S. F. (1970). "Gradation and shear characteristics of four cohesionless soils." *Can. Geotech. J.*, 7(1), 62–68.
- Stuedlein, A. W., Allen, T. M., Holtz, R. D., and Christopher, B. R. (2012). "Assessment of reinforcement strains in very tall mechanically stabilized earth walls." *J. Geotech. Geoenviron. Eng.*, 10.1061/(ASCE)GT.1943-5606.0000586, 345–356.
- Stuedlein, A. W., Bailey, M. J., Lindquist, D. D., Sankey, J., and Neely, W. (2010). "Design and performance of a 46-m-high MSE wall." *J. Geotech. Geoenviron. Eng.*, 10.1061/(ASCE)GT.1943-5606.0000294, 786–796.
- Stuedlein, A. W., Mikkelsen, P. E., and Bailey, M. J. (2007). "Instrumentation and performance of the third runway north MSE wall at Seattle-Tacoma international airport." *7th Int. Symp. on Field Measurements in Geomechanics, FMGM 2007*, ASCE, Reston, VA, 26.
- Suzuki, K. and Yanagisawa, E. (2006). "Principal deviatoric strain increment ratios for sand having inherent transverse isotropy." *Int. J. Geomech.*, 10.1061/(ASCE)1532-3641(2006)6:5(356), 356–366.
- Tatsuoka, F. (1976). "Stress-dilatancy relations of anisotropic sands in three dimensional stress condition." *Soils Found.*, 16(2), 1–18.
- Tatsuoka, F. (1987). "Discussion of 'The strength and dilatancy of sands' by Bolton, 1986." *Geotechnique*, 37(2), 219–226.
- Tatsuoka, F., Sakamoto, M., and Kawamura, T. (1986). "Strength and deformation characteristics of sand in plane strain compression at extremely low pressures." *Soils Found.*, 26(1), 65–84.
- Taylor, D. W. (1948). *Fundamentals of soil mechanics*, Wiley, New York.
- Terzaghi, K., Peck, R. B., and Mesri, G. (1996). *Geotechnique*, 3rd Ed., Wiley, London.
- Walters, J. J. (2013). "Characterization of reinforced fill soil, soil-reinforcement interaction and global stability of very tall MSE walls." M.S. thesis, Oregon State Univ., Corvallis, OR.
- Wan, R. G. and Guo, P. J. (2004). "Stress-dilatancy and fabric dependencies on sand behavior." *J. Eng. Mech.*, 10.1061/(ASCE)0733-9399(2004)130:6(635), 635–645.
- Wanatowski, D. and Chu, J. (2008). "Stress-strain behavior of a granular fill measured by a new plane-strain apparatus." *Geotech. Test. J.*, 29(2), 1–9.
- Wood, D. M. (1990). *Soil behaviour and critical state soil mechanics*, Cambridge University Press, Cambridge, U.K., 462.
- Xiao, Y., Liu, H., Chen, Y., and Jiang, J. (2014). "Strength and deformation of rockfill material based on large-scale triaxial compression tests. I: Influences of density and pressure." *J. Geotech. Geoenviron. Eng.*, 10.1061/(ASCE)GT.1943-5606.0001176, 04014070.
- Zhao, H. F., Zhang, L. M., and Chang, D. S. (2013). "Behavior of coarse widely graded soils under low confining pressures." *J. Geotech. Geoenviron. Eng.*, 10.1061/(ASCE)GT.1943-5606.0000755, 35–48.
- Zienciewicz, O. C., Humpheson, C. and Lewis, R. W. (1975). "Associated and non-associated visco-plasticity and plasticity in soil mechanics." *Geotechnique*, 25(4), 671–689.

Erratum for “Stress-Strain Response and Dilatancy of Sandy Gravel in Triaxial Compression and Plane Strain” by Andrew Strahler, Armin W. Stuedlein, and Pedro W. Arduino

DOI: 10.1061/(ASCE)GT.1943-5606.0001435

Andrew Strahler, S.M.ASCE

Graduate Research Assistant, School of Civil and Construction Engineering, Oregon State Univ., 101 Kearney Hall, Corvallis, OR 97331.

Armin W. Stuedlein, Ph.D., P.E., M.ASCE

Associate Professor, School of Civil and Construction Engineering, Oregon State Univ., 101 Kearney Hall, Corvallis, OR 97331 (corresponding author). E-mail: Armin.Stuedlein@oregonstate.edu

Pedro W. Arduino, Ph.D., P.E., M.ASCE

Professor, Dept. of Civil and Environmental Engineering, Univ. of Washington, 201 More Hall, Box 352700, Seattle, WA 98195-2700.

During the analysis of additional true triaxial data, the authors identified some errors in the computation of the shear modulus and shear strain in this manuscript that require the updating of several figures and revision of some conclusions. Engineering shear strains were incorrectly calculated for the PSK₀CD test specimens and did not reflect projection onto the deviatoric plane in accordance with Eq. (5). Accordingly, the previously published shear strains should be multiplied by $\sqrt{2}$ throughout the paper and in the original Figs. 7, 9, 11, 12, and 13. This error also requires adjustments to the PSK₀CD dilation angles and initial shear modulus as presented in Figs. 4, 10, and 14. The dilation angles presented in the revised Fig. 4 are 30% lower than those previously reported and now range from 30 to 16°. The dilation angle at the smallest

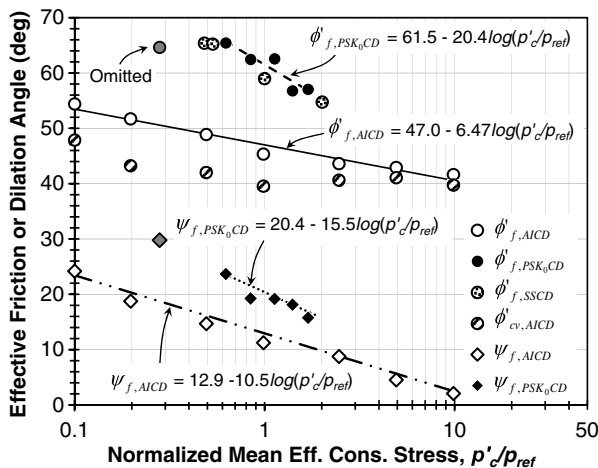


Fig. 4. Effective friction and dilation angles at failure as a function of normalized mean effective stress for AICD and PSK₀CD tests; gray-shaded points were removed from the PSK₀CD trends because of apparent boundary condition effects at low confining stresses

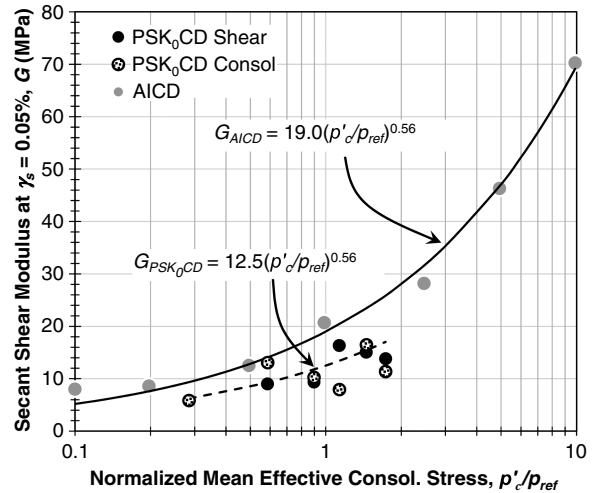


Fig. 10. Initial tangent shear modulus computed at 0.05% shear strain for AICD and PSK₀CD stress paths

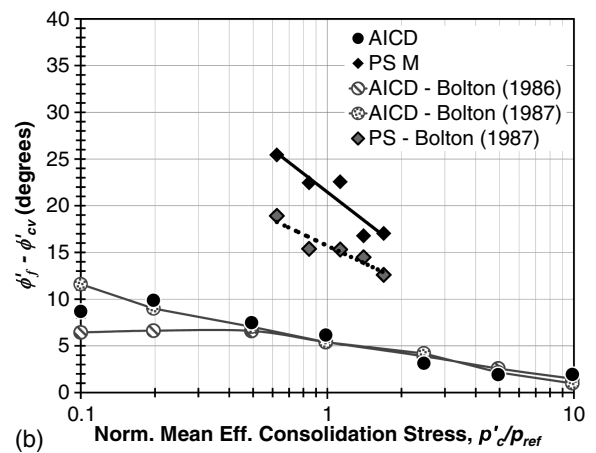
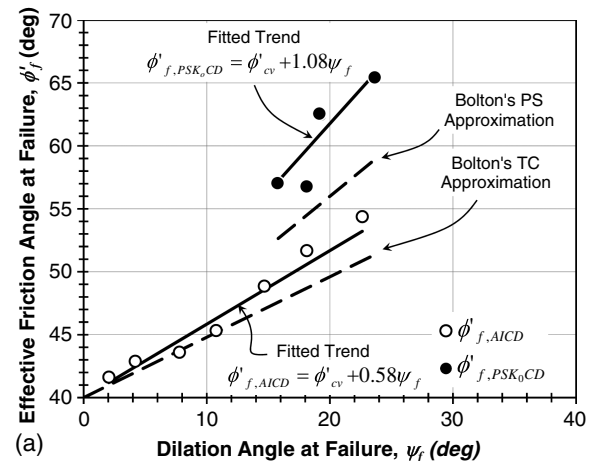


Fig. 14. Stress-dilatancy behavior of Kanaskat gravel: (a) comparison of effective friction and dilation angle at failure; (b) comparison of observations to Bolton's approximation as a function of mean effective confining stress

Downloaded from ascelibrary.org by OREGON STATE UNIVERSITY on 08/09/16. Copyright ASCE. For personal use only; all rights reserved.

confining pressure was omitted from the trend fitting because of apparent influences of boundary conditions at low confining stresses.

As described above, the revised shear strains required updates to the reported shear modulus, G_{PSK_0CD} . G_{PSK_0CD} must also be computed in the same manner as for the AICD stress path [i.e., $G = \Delta q / (3\Delta\gamma_s)$] and, therefore, the revised G_{PSK_0CD} must be $3\sqrt{2}$ smaller than previously reported. The initial PSK_0CD shear modulus presented in the revised Fig. 10 has been corrected for stress path and shear strain calculation errors. The revised G_{PSK_0CD} values are lower than those measured in the AICD stress path, which is not consistent with the plane strain shear modulus reported by others [e.g., (Hatami and Bathurst 2005)].

To explore this finding, the consolidation-phase shear strains developed during the K_0 stress path were used to estimate the shear modulus near the end of the consolidation phase. The shear modulus calculated at the end of consolidation, presented alongside the G_{PSK_0CD} in the revised Fig. 10, is similar to that measured at the onset of shearing. This confirms that the soil behavior is independent of the stress path. We conclude that the low magnitudes of the revised G_{PSK_0CD} are attributed to the development of small magnitudes of ε_2 strains that stem from the displacements in the load cells in the intermediate direction. During consolidation, ε_2 was

observed to be 0.03% on average and ranged from 0.02 to 0.06%. Therefore, the intermediate principal strains that develop within the UW-TTA system may not be small enough to accurately represent a true plane strain condition at small strains as a result of system compliance.

The revised Fig. 14 presents the corrected stress-dilatancy response of Kanaskat gravel, indicating that Bolton's (1986) stress-dilatancy approximation underestimates the magnitude of dilation in well-graded gravelly soils by 22% on average. The revised comparison suggests that the plane strain stress-dilatancy response of well-graded gravelly soils at failure exhibits greater dilatancy than that predicted by Bolton's (1986) approximation, which represents a new conclusion stemming from these data.

References

- Bolton, M. D. (1986). "The strength and dilatancy of sands." *Geotechnique*, 36(1), 65–78.
- Hatami, K., and Bathurst, R. J. (2005). "Development and verification of a numerical model for the analysis of geosynthetic reinforced soil segmental walls under working stress conditions." *Can. Geotech. J.*, 42(4), 1066–1085.